



## T cell receptor assessment in autoimmune disease requires access to the most adjacent immunologically active organ



Bergithe E. Oftedal <sup>a, b, \*, 1</sup>, Brita Ardesjö Lundgren <sup>a, c, 1</sup>, David Hamm <sup>d</sup>, Poh-Yi Gan <sup>e</sup>, Stephen R. Holdsworth <sup>e</sup>, Christopher N. Hahn <sup>a, i</sup>, Andreas W. Schreiber <sup>f, i</sup>, Hamish S. Scott <sup>a, f, g, h, i, \*\*</sup>

<sup>a</sup> Department of Genetics and Molecular Pathology, Centre for Cancer Biology, An Alliance Between SA Pathology and the University of South Australia, Adelaide, Australia

<sup>b</sup> Department of Clinical Science, University of Bergen, Norway

<sup>c</sup> Department of Medical Biochemistry and Microbiology, Uppsala University, Sweden

<sup>d</sup> Adaptive Biotechnologies, 1551 Eastlake Ave E #200, Seattle, WA, 98102, USA

<sup>e</sup> Centre for Inflammatory Diseases, Monash University Department of Medicine, Clayton, Australia

<sup>f</sup> ACRF Cancer Genomics Facility, Centre for Cancer Biology, SA Pathology, Adelaide, Australia

<sup>g</sup> School of Pharmacy and Medical Sciences, Division of Health Sciences, University of South Australia, Australia

<sup>h</sup> School of Biological Sciences, University of Adelaide, Australia

<sup>i</sup> School of Medicine, University of Adelaide, Adelaide, Australia

### ARTICLE INFO

#### Article history:

Received 22 November 2016

Received in revised form

28 February 2017

Accepted 6 March 2017

Available online 18 March 2017

#### Keywords:

Next generation sequencing

T cell receptor repertoire

Autoimmune regulator

### ABSTRACT

Next generation sequencing of T and B cell receptors is emerging as a valuable and effective method to diagnose and monitor hematopoietic malignancies. So far, this approach has not been fully explored in regard to autoimmune diseases. T cells develop in the thymus where they undergo positive and negative selection, and the autoimmune regulator (Aire) is central in the establishment of immunological tolerance. Loss of Aire leads to severe multiorgan autoimmune disease with infiltration of autoreactive T cells in affected organs. Here, we have utilized next generation sequencing technology to investigate the T cell receptor repertoire in autoimmunity induced by immunization of mice with a self-antigen, myeloperoxidase. By investigating the T cell receptor repertoire in peripheral blood, spleen and lumbar lymph nodes from naïve and immunized Aire  $-/-$  mice and wild type littermates, changes in the usage of V and J genes were evident. Our results identify TCR clonotypes which could be potential targets for immune therapy. Also, Aire  $-/-$  autoimmunity is driven by a variety of autoantigens where the autoimmune response is highly polyclonal, and access to the most adjacent immunologically active tissue is required to identify T cell receptor sequences that are potentially unique to the antigen in Aire  $-/-$  immunized mice.

© 2017 The Authors. Published by Elsevier Ltd. This is an open access article under the CC BY-NC-ND license (<http://creativecommons.org/licenses/by-nc-nd/4.0/>).

### 1. Introduction

Next generation immunosequencing allows for detailed identification and quantitation of every T cell in a biologic sample. This

\* Corresponding author. Department of Clinical Science, University of Bergen, 5021, Bergen, Norway.

\*\* Corresponding author. Department of Genetics and Molecular Pathology, Centre for Cancer Biology, SA Pathology, PO Box 14, Rundle Mall, Adelaide, 5000, South Australia, Australia.

E-mail addresses: [Bergithe.oftedal@uib.no](mailto:Bergithe.oftedal@uib.no) (B.E. Oftedal), [hamish.scott@sa.gov.au](mailto:hamish.scott@sa.gov.au) (H.S. Scott).

<sup>1</sup> Equal contribution.

enables the assessment of clonal expansion and the detection of shared clones among multiple samples of interest and has become an appreciated method to monitor and diagnose haematological malignancies [1,2], but so far this technology has been less investigated in autoimmune diseases [3].

Effective T cell immunity relies on the enormous diversity of their membrane bound T cell receptor (TCR) repertoire. The combinatorial diversity generated by the V(D)J recombination mechanisms in the thymus results in the somatically hypervariable CDR3 loop recognising the peptide antigen presented by major histocompatibility complexes I and II [4,5]. T cells undergo positive and negative selection in the thymus, where the autoimmune

regulator (Aire), a mediator of negative selection, is essential for the establishment of immune tolerance [6]. Aire is mainly expressed in a subset of medullary thymic epithelial cells (mTECs), allowing the promiscuous expression of peripheral antigens to be displayed to developing T cells [7,8].

In humans, the lack of AIRE leads to multiorgan autoimmune disease [9,10], where the endocrine organs, like the adrenals and the parathyroid glands are affected in particular [11]. The infiltration of T cells is evident in the affected organs, and patients also develop high levels of circulating autoantibodies directed against proteins expressed in the affected tissues. Although this is a rare disease, it has been valuable in studying the mechanisms behind a functional immune system and the impact of negative selection [12,13]. C57BL/6 mice mimicking a human 13-base pair AIRE deletion were shown to have altered development of their mTECs and a mild autoimmune phenotype with infiltrating T cells in affected organs particularly the eyes and salivary glands [14]. Previous assessment of T cells in these mice has shown minimal changes in the TCR repertoire and a polyclonal expansion of autoreactive T cells [14].

The expression of myeloperoxidase (MPO) was found to be under Aire control in thymus [15]. The role of systemic autoimmunity to MPO in the development of crescentic glomerulonephritis has been unraveled during the last years, where both antibody producing B cells [16] and MPO specific T cells have been shown to be important for the disease development [17,18]. In Aire  $-/-$  mice immunized with MPO, increased frequencies of anti-MPO CD4<sup>+</sup> T effector cells resulted and the severity of glomerulonephritis was enhanced [15]. This has now become a validated model of MPO-induced autoimmunity, where the T cells have been shown to direct disease progression [17–21].

We used next generation sequencing to study the TCR repertoire in autoimmunity by exploring the expansion and specificity of autoreactive T cells in naïve and MPO immunized mice that were either intact or had lack of negative selection (Aire deficiency). The rearranged TCR $\beta$  CDR3 regions were sequenced in peripheral blood and from the immunological active organs spleen and lumbar lymph nodes (LNs) in all groups of mice. Using this as a model system, we hypothesized that the MPO-immunization would change the V and J gene usage and increase the number of overlapping CDR3 sequences in both Aire  $-/-$  and wt mice, and aimed to explore the potential of the TCR repertoire as a diagnostic marker for autoimmune diseases.

We here found specific V and J genes upregulated in MPO immunized wt and Aire  $-/-$  mice and a lack of clonal increase in the Aire  $-/-$  mice which suggests that the autoimmunity is driven by a wide variety of antigens. The TCR $\beta$  sequences likely to be MPO-specific were more easily detected in LN samples after immunization, and hardly ever seen in samples from peripheral blood. Our findings suggest that the individual responses towards autoantigens are unique and polyclonal, and highlight the importance of selecting the relevant tissue to assess if analysis of the TCR repertoire is to be utilized in the monitoring of immunization and autoimmune diseases.

## 2. Materials and methods

### 2.1. Mice and MPO induction

Mice of the Aire  $-/-$  and  $+/+$  genotype on the C57BL/6 background were used (Hubert et al. [14]). Mice were bred at the animal house at the Center for Cancer Biology, Adelaide, Australia and immunization experiments were performed at the Monash Medical Center Animal Facility, Melbourne, Australia, according to the animal ethics guidelines. Aire  $-/-$  and control Aire  $+/+$  (wt) male

littermates ( $n = 7$  and  $n = 4$ , respectively) were immunized with 20  $\mu$ g of native mouse MPO (nmMPO) [22] in Freund's complete adjuvant subcutaneously at the base of tail at Day 0. At Day 7, the mice were immunized again with 20  $\mu$ g nm MPO in Freund's incomplete adjuvant subcutaneously at the neck. Nine days after immunization, glomerulonephritis was induced in all mice by planting endogenous MPO in their glomeruli using an established technique [18,20,21] of administering 1.5 mg of sheep anti-mouse GBM globulin intravenously on two consecutive days. Mice were humanely culled at day 20. As controls for the TCR $\beta$  sequencing, naïve Aire  $-/-$  and  $+/+$  mice were used ( $n = 5$  in each group). Unfortunately, we did not get good quality DNA from spleen from one of the immunized Aire  $-/-$  mice, and in the group of naïve wt mice DNA from peripheral blood and lymph nodes were not available from one mouse. Mice were age matched to the immunized mice, the majority of the mice being 16 or 17 weeks of age at date of death while two immunized Aire  $-/-$  and one mouse in each of the naïve groups were 28–29 weeks at date of death. The mice were also sex matched except for the use of one female mouse in each of the naïve groups. Freund's adjuvant contains many immunogenic foreign proteins and using it does generate many antigen specific immune responses. However, trying to induce autoimmunity, adjuvants are essential in the complex processes that results in the loss of tolerance and broadly accepted as being necessary for the generation of adaptive immunity. We have previously shown in this model that MPO immunized Aire  $-/-$  mice develop more severe anti-MPO GN compared to MPO immunized WT mice. The measures of glomerular injury included functional renal loss (measured by the extent of albumin leakage, albuminuria) and structural renal damage (quantitated by the frequency glomerular focal segmental necrosis and the extent of injurious lymphocyte infiltration into the glomeruli). All measures were significantly more severe in MPO immunized Aire  $-/-$  mice than WT mice [15].

### 2.2. DNA extraction

Spleens and lumbar lymph nodes were harvested and snap frozen in liquid nitrogen. Peripheral blood (200–500  $\mu$ l) was collected by cardiac puncture, thoroughly mixed with 50  $\mu$ l of 0.5M EDTA pH 8.0 and snap frozen in liquid nitrogen. DNA was extracted using the QIAamp DNA Mini kit from QIAGEN according to the instructions for blood and tissue samples respectively.

### 2.3. TCR $\beta$ CDR3 sequencing

Amplification and sequencing of the TCR $\beta$  CDR3 regions was performed by Adaptive technologies using protocols described previously by Robins et al. [23]. Briefly, a multiplexed PCR method was employed to amplify all possible rearranged genomic TCR $\beta$  sequences in mice using 34 forward primers, each specific to a functional TCR V $\beta$  segment, and 14 reverse primers, each specific to a TCR J $\beta$  segment. LN samples with an estimated input of 200,000 T cell genomes were sequenced to get a targeted output of 800,000 sequences. Spleen and blood samples with an estimated input of 40,000 T cell genomes were sequenced to reach a target output of 200,000 sequences. The total number of sequences for LN samples was higher than the expected output of 800,000 sequences while a few spleen samples and half of the blood samples were below the expected output of 200,000 sequences. The divergence in sequence output could be due to differences in the number of input T cells, and a lower percentage of TCR genomes than expected in some of the samples.

**Table 1**  
TCR $\beta$  CDR3 deep sequencing result for lymph node (LN) samples.

| Original Sample | Geno-type | Immunized with MPO | Productive DNA sequences | Non-productive DNA sequences | Total DNA sequences | Unique productive DNA sequences | Unique productive aa sequences | Total unique sequences | Unique V-gene J-gene combinations | Fraction of unique vs. total unique sequences | Clonality |
|-----------------|-----------|--------------------|--------------------------|------------------------------|---------------------|---------------------------------|--------------------------------|------------------------|-----------------------------------|---|-----------|
| LN1735          | +/+       | +                  | 1 991 274                | 892 022                      | 2 883 296           | 31 630                          | 28 911                         | 48 688                 | 302                               | 65,0  | 0,08      |
| LN1736          | +/+       | +                  | 935 462                  | 392 179                      | 1 333 556           | 25 881                          | 23 884                         | 39 571                 | 290                               | 65,4  | 0,07      |
| LN1737          | +/+       | +                  | 2 058 899                | 820 170                      | 2 879 069           | 38 308                          | 34 670                         | 59 207                 | 307                               | 64,7  | 0,13      |
| LN1738          | +/+       | +                  | 1 764 655                | 675 753                      | 2 440 408           | 39 132                          | 35 554                         | 60 654                 | 314                               | 64,5  | 0,09      |
| LN1739          | -/-       | +                  | 1 780 190                | 692 027                      | 2 484 108           | 54 229                          | 48 576                         | 83 854                 | 306                               | 64,7  | 0,07      |
| LN1740          | -/-       | +                  | 1 342 025                | 576 843                      | 1 918 868           | 42 286                          | 38 276                         | 65 182                 | 303                               | 64,9  | 0,08      |
| LN1741          | -/-       | +                  | 719 656                  | 298 042                      | 1 017 698           | 30 448                          | 28 066                         | 46 251                 | 296                               | 65,8  | 0,09      |
| LN1742          | -/-       | +                  | 3 052 632                | 1112 693                     | 4 165 325           | 21 853                          | 20 130                         | 34 436                 | 299                               | 63,5  | 0,07      |
| LN1743          | -/-       | +                  | 2 557 834                | 1016 103                     | 3 573 937           | 35 408                          | 32 149                         | 55 684                 | 309                               | 63,6  | 0,07      |
| LN1744          | -/-       | +                  | 3 462 945                | 1293 215                     | 4 756 160           | 43 328                          | 38 796                         | 69 130                 | 311                               | 62,7  | 0,06      |
| LN1745          | -/-       | +                  | 1 965 343                | 785 710                      | 2 751 053           | 42 034                          | 37 809                         | 65 307                 | 315                               | 64,4  | 0,08      |
| LN2             | -/-       | -                  | 999 985                  | 421 973                      | 1 421 958           | 30 899                          | 28 464                         | 47 973                 | 294                               | 64,4  | 0,07      |
| LN71            | -/-       | -                  | 1 599 834                | 704 541                      | 2 304 375           | 21 411                          | 19 871                         | 33 567                 | 297                               | 63,8  | 0,15      |
| LN72            | -/-       | -                  | 1 170 172                | 505 708                      | 1 675 880           | 29 076                          | 26 800                         | 45 035                 | 290                               | 64,6  | 0,06      |
| LN74            | -/-       | -                  | 1 639 616                | 669 818                      | 2 309 434           | 32 540                          | 29 620                         | 51 009                 | 295                               | 63,8  | 0,07      |
| LN75            | -/-       | -                  | 931 447                  | 389 591                      | 1 321 038           | 33 750                          | 30 930                         | 51 680                 | 292                               | 65,3  | 0,07      |
| LNc57Na         | +/+       | -                  | 3 267 878                | 1334 592                     | 4 602 470           | 35 139                          | 31 981                         | 56 211                 | 302                               | 62,5  | 0,06      |
| LN54            | +/+       | -                  | 3 345 378                | 1235 426                     | 4 580 804           | 91 797                          | 81 033                         | 144 839                | 325                               | 63,4  | 0,07      |
| LN70            | +/+       | -                  | 1 005 888                | 393 194                      | 1 399 082           | 18 534                          | 17 397                         | 28 007                 | 278                               | 66,2  | 0,18      |
| LN83            | +/+       | -                  | 3 033 738                | 1251 284                     | 4 285 022           | 34 984                          | 31 544                         | 54 834                 | 309                               | 63,8  | 0,09      |

#### 2.4. Identification of TCR $\beta$ CDR3 sequences and VDJ decomposition

Raw Illumina sequence reads were demultiplexed based upon Adaptive's proprietary barcodes then further processed to remove adapter and primer sequences, primer dimer, germline and other contaminant sequences. The data is then filtered and clustered using both the relative frequency ratio between similar clones and a modified nearest-neighbour algorithm, to merge closely related sequences introduced through PCR and sequencing. The resulting sequences were sufficient to allow annotation of the V(N)D(N)J genes constituting each unique CDR3 and the translation of the encoded CDR3 amino acid sequence. V, D and J gene definitions were based on annotation in accordance with the IMGT database ([www.imgt.org](http://www.imgt.org)). The set of observed biological TCR beta CDR3 sequences were normalized to correct for residual multiplex PCR amplification bias and quantified against a set of synthetic TCR beta CDR3 sequence analogues. TCR $\beta$  CDR3 region was identified according to the definition previously established by the International [24].

#### 2.5. Overlap in unique sequences between two mice

Clones in common between mice within and between groups were compared using their relative frequencies.

#### 2.6. Identification of TCR $\beta$ CDR3 sequences specifically increased in mice immunized with MPO

To identify the TCR $\beta$  CDR3 sequences that were specifically increased in response to MPO induction we compared the abundance distribution of clones across the 7 immunized ko mice (LN samples) to the binomial distribution that one would expect if all clones were randomly drawn from a common population with equal probability. These distributions diverged for MPO-specific clones that were present in more than approx. 4 out of the total of 7 mice, so we considered clones present in 4 or more clones as potentially MPO-induced.

Clones that were considered potentially specific for MPO were present in a number of immunized ko mice above the cut off and could be present in immunized wt and naïve ko mice but not in any tissue samples from naïve wt mice. By not including any cloned

found in naïve wt mice, most native public clones were eliminated. Clones present at 2 copies or above was considered possibly expanded (communication with Adaptive technologies). The resulting list of clones was ranked by their total number across the 7 immunized ko mice, and normalized by the total depth per sample (weighted average number).

The edit distance analysis in the Immuno Seq analyser software was used to identify clones differing in only one aa from the top clone in common between immunized mice. Clones that were present in naïve wt mice or only present in naïve ko mice were excluded.

The TCR $\beta$  CDR3 sequences for the top 10 potentially MPO specific clones in common for immunized mice as well as the top 5 sequences in common for ko mice were blasted using WU-BLAST, an implementation of the Basic Local Alignment Search Tool (BLAST) by Altschul et al. [25], at the Mouse Genome Informatics Web Site, URL: <http://www.informatics.jax.org> (March, 2013). They were also blasted against the Genbank Mouse database and the UniProt Mouse database (March 2013), and analysed using IMGT/V-QUEST [26] on the Immunogenetics Web Site URL: <http://www.imgt.org> (September, 2016).

#### 2.7. Statistical analysis

All statistical analyses were performed using GraphPad Prism 5 software (La Jolla, USA). Student's t-test was used when comparing two groups and 1-way Anova with the Bonferroni's test for multiple comparisons when more than two groups were compared. P-values below 0.05 were considered statistically significant.

### 3. Results

#### 3.1. TCR $\beta$ CDR3 sequencing

Rearranged TCR $\beta$  CDR3 regions in genomic DNA samples from LNs, spleen and peripheral blood from Aire -/- and wt mice either naïve or immunized with MPO, were sequenced using the immunoSEQ assay (Adaptive biotechnologies, Seattle, Washington). Between 700,000 and 3,4 million TCR $\beta$  CDR3 in-frame sequence reads from the LN samples were generated (Table 1), while fewer sequence reads for spleen and blood samples were obtained; with

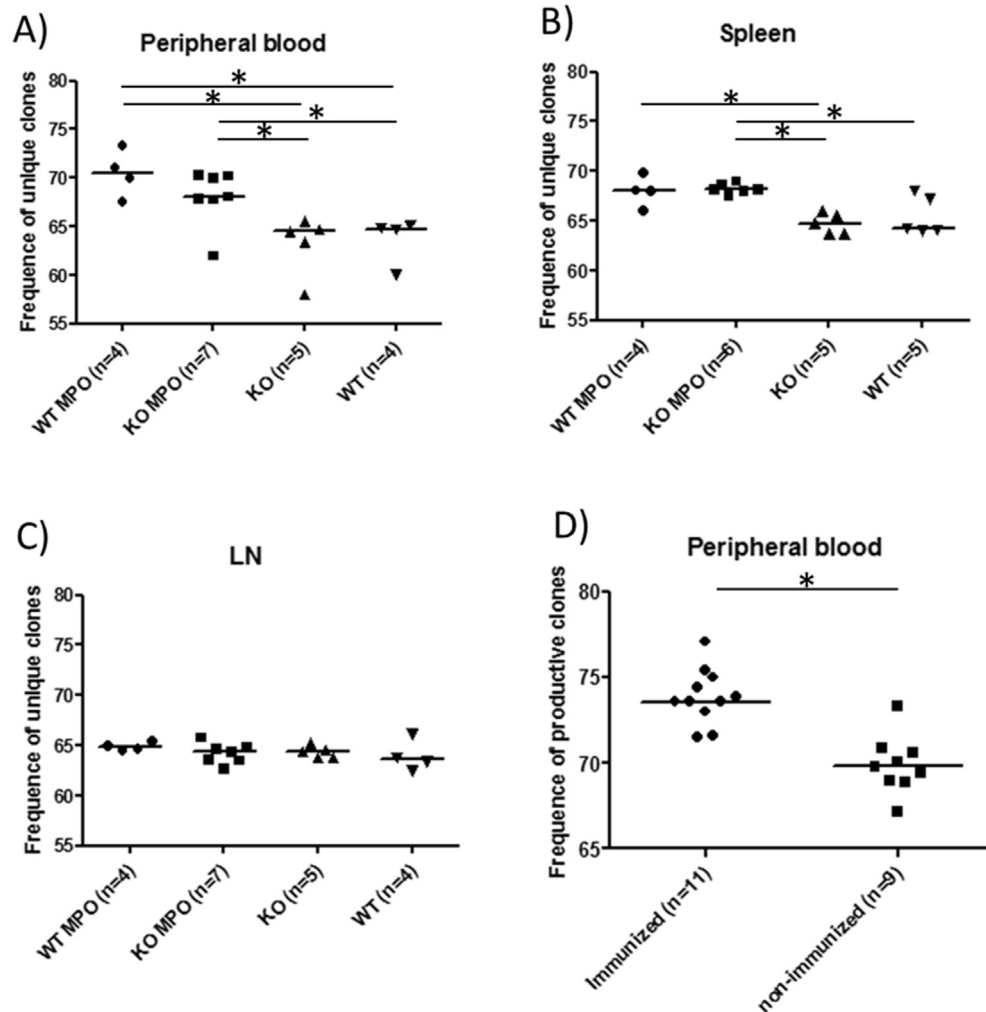


**Fig. 1. Frequency of unique clones.** The ratio of unique versus total unique sequences is shown for all groups in peripheral blood (A), spleen (B) and LN (C). The ratio between the immunized and the naïve groups of mice is shown in (D). Median is shown for all groups. \* $p < 0.05$ .

75,000–1,400,000 and 6000–1,200,000 respectively (Supplementary Tables S1 and S2).

As a measure of diversity, we elected to use the ratio of productive unique to total sequences (Fig. 1), productive sequences being sequences within reading-frame and without stop. In both spleen and peripheral blood, the amount of unique productive sequences were significantly higher ( $p < 0.05$ ) in MPO immunized mice compared to non-immunized mice. However, no differences between the groups were found in LN samples or between Aire  $-/-$  and wt mice. To what extent the repertoire was dominated by one or a few clones (clonality) was investigated in the productive sequences but no differences were found between the four groups of mice in any of the tissues (data not shown).

### 3.2. TCR $\beta$ V- and J gene utilization

For the productive sequences, the V $\beta$  gene usage was distributed similarly in the different tissues among the different groups of mice (Fig. 2 and Supplementary Fig. S1). The immunization with MPO reflected on the repertoire by changing the V $\beta$  gene utilization. Most profound were the differences in the V families V $\beta$  3, 5, 12, 13, 14, 17, 19, and 29 between the immunized and the naïve mice (Supplementary Figs. S1 and S2). In particular, the individual V gene with largest difference in utilization between immunized and naïve

mice in all tissues was 13-3 ( $p < 0.01$ ) (Fig. 2). This suggests this gene to be used in clones specifically expanded in response to MPO immunization, and several of the clones with the highest copy numbers in common for immunized mice actually used the 13-3 V $\beta$  gene (Table 2). The differences in the V $\beta$  usage was not as profound when comparing naïve Aire  $-/-$  mice to the two wt groups, but there was a significantly higher utilization of V genes 3-0, 17-0 and 19-0 in naïve Aire  $-/-$  mice in the three tissues investigated ( $p < 0.01$ ) (Fig. 2). This suggests that these V genes are likely to be utilized in TCR clones bearing receptors that recognise self-antigens related to Aire-deficiency.

The differences between the groups were smaller for the J gene than for the V gene usage, but some differences were significant in the LN samples (Supplementary Fig. S3). Here naïve Aire  $-/-$  mice had higher usage of some J genes, e.g. J 2-3. This might suggest a difference in expanded TCR clones due to Aire deficiency. The utilization of J gene 2-3 was also more similar between the two Aire  $-/-$  groups in the spleen and peripheral blood samples, which supports the idea of a specific J gene usage in Aire deficient mice.

In total, there were 34 V genes and 14 J genes used in all LN samples, hence a total of 476 combinations were available. Among the LN samples only 378 of these combinations appeared which could suggest a biased usage of V and J genes.

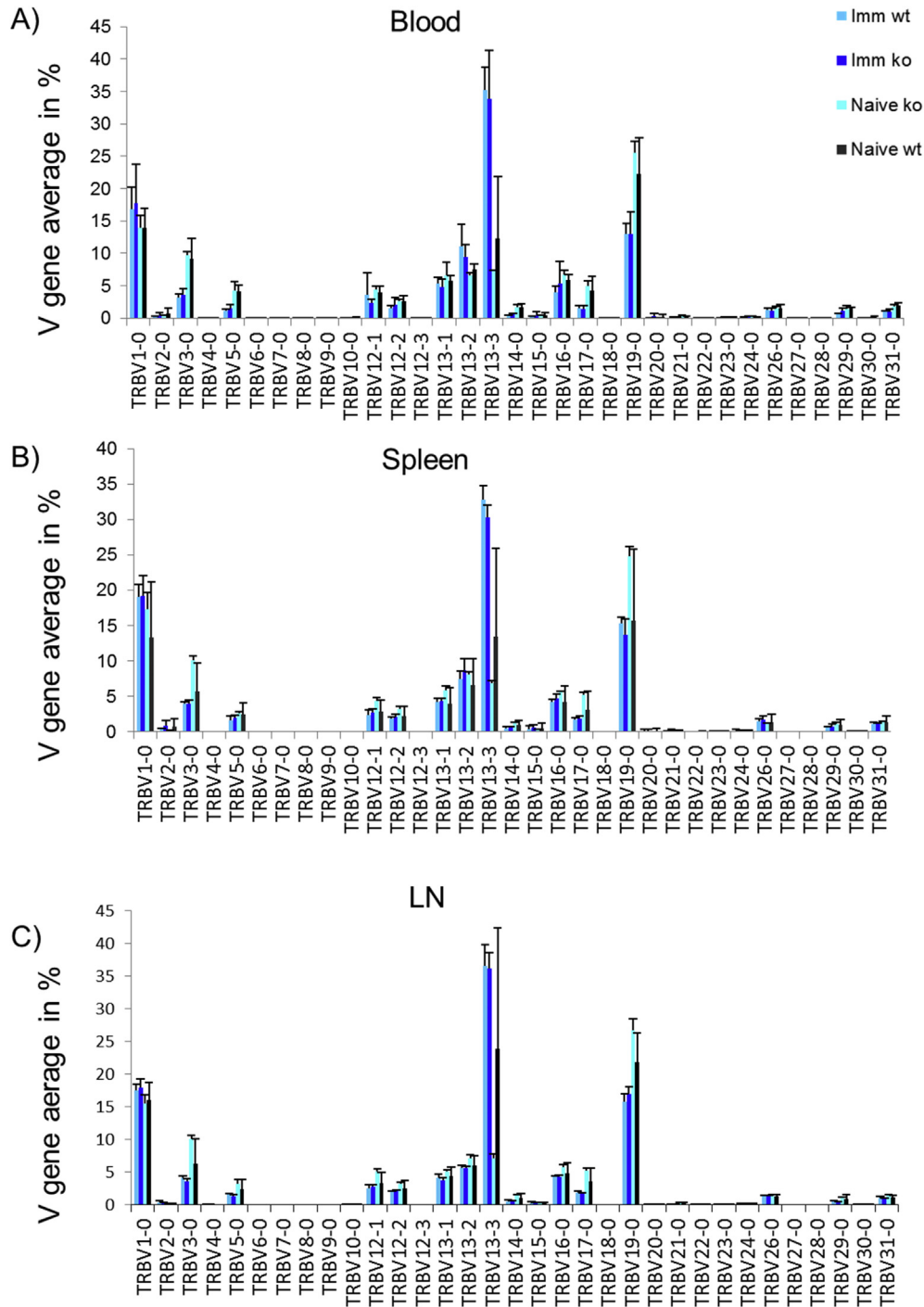


**Fig. 2. The frequency of V genes for all tissues.** The mean value of the frequencies of the individual V gene usage per sample is shown for peripheral blood (A), spleen (B) and lymph node (C). 13–3 is the V-gene with most profound change between the immunized and the naïve mice ( $p < 0.01$ ). Comparing naïve Aire  $-/-$  mice to the two wt groups, 3–0, 17–0 and 19–0 were significantly higher in naïve Aire  $-/-$  mice in all tissues ( $p < 0.01$ ). The standard deviation is shown for all groups.

### 3.3. Overlap of TCR $\beta$ CDR3 repertoire

We found the overlap of unique nucleotide sequences between all samples to be tissue-dependent, and dependent on the depth of the sequencing, when assessing the overall overlap between the groups. The highest number of overlapping nucleotide sequences was seen in LN and spleen samples, where all twenty samples shared a single clone, while this was reduced to only 14 mice sharing one clone in peripheral blood (Fig. 3). Of note, spleen and

peripheral blood were sequenced to the same depth, which highlights the tissue-effect.

Analysing the overlapping unique amino acid sequences within the four groups, we expected the immunized and the Aire  $-/-$  mice to have more clones in common as they develop immunity to shared antigens. For the LN samples, it seems like the overlap of unique clones was mostly dependent on the number of samples investigated, and in peripheral blood there was hardly any overlap in any of the groups (0–2 shared clones) (Fig. 4). However, looking

**Table 2**

Top clones present in common in immunized and Aire ko mice.

|       | Amino acid sequence of CDR3 region | V    | D | J   | Copies for IKOs LN <sup>a</sup> | Copies in LNs IM | IKO with clones in LN (n = 7) | IWT with clones in LN (n = 4) | Copies in NKOs LNs | NKO with Clones in LN (n = 5) | Copies in spleen | IKO with clones in spleen (n = 6) | IWT with clones in spleen (n = 4) | NKO with clones in spleen (n = 5) | Copies in blood | Mice with clones in blood (n = 16) |
|-------|------------------------------------|------|---|-----|---------------------------------|------------------|-------------------------------|-------------------------------|--------------------|-------------------------------|------------------|-----------------------------------|-----------------------------------|-----------------------------------|-----------------|------------------------------------|
| IM/KO | <u>C</u> ASSGTENTEVFF              | 13–1 | 1 | 1–1 | 1063,2                          | 10451            | 7                             | 4                             | 24                 | 1                             | 488              | 5                                 | 2                                 | 0                                 | 7               | 1 <sup>b</sup>                     |
|       | <u>C</u> ASRDISNERLFF              | 13–3 | 1 | 1–4 | 741,5                           | 9712             | 4                             | 1                             | 0                  | 0                             | 63               | 1                                 | 1                                 | 0                                 | 12              | 1 <sup>b</sup>                     |
|       | <u>C</u> ASSITGENTLYF              | 19–0 | 1 | 2–4 | 343,9                           | 1815             | 5                             | 1                             | 0                  | 0                             | 165              | 3                                 | 1                                 | 1                                 | 33              | 1 <sup>b</sup>                     |
|       | <u>C</u> ASGTHNNQAPLF              | 13–2 | 1 | 1–5 | 245,2                           | 2499             | 4                             | 1                             | 0                  | 0                             | 82               | 1                                 | 0                                 | 0                                 | 0               | 0                                  |
|       | <u>C</u> ASGDHSNSDYTF              | 13–2 | 1 | 1–2 | 229,3                           | 1257             | 5                             | 2                             | 0                  | 0                             | 82               | 3                                 | 2                                 | 0                                 | 2               | 1 <sup>b</sup>                     |
| IKO   | <u>C</u> ASSEGNTVEVF               | 13–3 | 1 | 1–1 | 227,9                           | 1792             | 5                             | 2                             | 0                  | 0                             | 52               | 0                                 | 1                                 | 0                                 | 0               | 0                                  |
|       | <u>C</u> ASSTGGAETLYF              | 19–0 | 1 | 2–3 | 889,8                           | 7146             | 5                             | 0                             | 0                  | 0                             | 775              | 2                                 | 0                                 | 0                                 | 0               | 0                                  |
|       | <u>C</u> ASSDTGGNTGQLYF            | 13–3 | 2 | 2–2 | 425,3                           | 4204             | 4                             | 0                             | 0                  | 0                             | 113              | 1                                 | 0                                 | 0                                 | 13              | 1 <sup>b</sup>                     |
|       | <u>C</u> ASSRDWANQDTQYF            | 19–0 | 2 | 2–5 | 316,9                           | 1459             | 4                             | 0                             | 0                  | 0                             | 0                | 0                                 | 0                                 | 0                                 | 20              | 1 <sup>b</sup>                     |
|       | <u>C</u> ASSGVQDTQYF               | 13–3 | 1 | 2–5 | 198,6                           | 1859             | 4                             | 0                             | 0                  | 0                             | 0                | 0                                 | 0                                 | 0                                 | 0               | 0                                  |
| KO    | <u>C</u> TCSAGQGTNERLFF            | 1–0  | 1 | 1–4 | 431,2                           | 3637             | 4                             | 0                             | 0                  | 0                             | 209              | 0                                 | 0                                 | 2                                 | 0               | 0                                  |
|       | <u>C</u> ASREISNERLFF              | 13–3 | 1 | 1–4 | 320,7                           | 1773             | 4                             | 0                             | 37                 | 1                             | 0                | 0                                 | 0                                 | 0                                 | 0               | 0                                  |
|       | <u>C</u> TCSADINQDTQYF             | 1–0  | 1 | 2–5 | 280,6                           | 1647             | 4                             | 0                             | 0                  | 0                             | 0                | 0                                 | 0                                 | 0                                 | 231             | 1 <sup>b</sup> 1 <sup>c</sup>      |
|       | <u>C</u> ASSDAGSQDTQYF             | 13–3 | 1 | 2–5 | 168,8                           | 1284             | 4                             | 0                             | 41                 | 2                             | 14               | 0                                 | 0                                 | 1                                 | 0               | 0                                  |
|       | <u>C</u> ASSANSDYTF                | 13–3 | 1 | 1–2 | 166,9                           | 788              | 4                             | 0                             | 7                  | 1                             | 0                | 0                                 | 0                                 | 0                                 | 0               | 0                                  |

LN: lymph node, IM: immunized mice (both groups), IKO: immunized knock out, IWT: immunized wild type, NKO: naïve knock out. In the amino acid sequence of the CDR3 region the first underlined amino acids indicate the V gene, the last ones the J gene.

Amino acids not underlined indicate D gene, nucleotides and transitions between genes.

<sup>a</sup> Weighted average number.

<sup>b</sup> IKO mouse.

<sup>c</sup> Indicates NKO mouse.

at the samples from spleen, it is evident that the immunization with MPO significantly ( $p < 0.05$ ) reduces the number of overlapping unique nucleotide sequences (Fig. 4D). This suggests an individual, polyclonal expansion toward this antigen, and underscores the importance of studying an immunologically active tissue.

In a pair-wise comparison of common clones within each group, the highest number of common clones was found in the naïve wt and immunized Aire  $-/-$  samples and the lowest number of common clones was seen in naïve Aire  $-/-$  mice (Table S3 and S4), which could suggest a polyclonal recognition of common autoantigens.

#### 3.4. Identification of TCR $\beta$ CDR3 sequences specifically increased in mice immunized with MPO

To identify the TCR $\beta$  CDR3 sequences specifically increased in response to MPO immunization, we investigated the LN samples, as this was the tissue with largest sample sizes and the MPO specific clones should be enriched in the draining LNs. The sequences were defined by demanding that the clones were (i) in common in four immunized mice (Supplementary Figure S4), (ii) not expanded in naïve wt mice, (iii) present at above 2 copies in a sample. These clones should be present in one or both the immunized groups, and could be detected in naïve Aire  $-/-$  mice as they have the propensity to develop autoimmunity to this antigen (Fig. 5). The resulting list of clones was further ranked by their total number across the 7 immunized Aire  $-/-$  mice, and normalized by the total depth per sample. The top clones are listed in Table 2, including a number of clones present at higher levels in one or more of the naïve Aire  $-/-$  mice, representing TCR clones possibly expanded in response to a common autoantigen.

The most interesting clone is comprised by the amino acid sequence CASSGTENTEVFF and utilizes the TRBV13-1 and TRBJ1-1 genes (Table 2). This clone had the highest collective copy number among the LN samples, and was present at high levels in the spleen samples, and in one blood sample. The likelihood of the same TCR arrangement being in two individuals and having a high

affinity toward the MPO antigen is unknown and could be low. Therefore, the other clones listed as potential clones in Table 2 could also be specifically expanded in response to the immunization with MPO. We also identified clones only present in Aire  $-/-$  mice, both immunized and naïve, which could be expanded in response to common autoantigens (Table 2).

The amino acid sequences in our top ten clones share some similarities. The two longest shared CDR3-motifs made up by the D gene and inserted nucleotides is G\_H\_N and TGG, and is shared by two of the top clones in immunized wt mice and immunized Aire  $-/-$  mice, respectively (Table 2). Investigating single amino acid substitutions in CDR3 of the top clone identified 5 potentially mutated clones, after elimination of clones present in naïve wt mice or at high levels in naïve Aire  $-/-$  mice. Of these, the clone most likely to be mutated and recognising the same antigen as the original top clone had the CDR3 sequence CASSETENTEVFF (Table S5), and was present in higher levels than the CASSGTENTEVFF clone in one immunized Aire  $-/-$  mouse.

The top ten TCR $\beta$  CDR3 sequences expanded in immunized mice and the top 5 sequences expanded in Aire  $-/-$  mice were blasted against the Genbank Mouse and the UniProt Mouse databases, to see if they are commonly expanded in mice. No clones had an identical match in either the nucleotide or the protein database. These sequences were also analysed using IMGT/V-QUEST. This program could correctly identify the V and J genes but not the D genes according to the programs requirements. For thirteen of the fifteen top clones the best match using the IMGT/V-QUEST was however identical to the D gene identified by the sequencing analysis tool, which is in fact based on annotation in accordance with the IMGT database. No TCR $\beta$  CDR3 sequence show perfect alignment with any sequences in the databases, as would be expected for a novel finding.

#### 4. Discussion

In this study, we have investigated the utility of next generation sequencing of the TCR repertoire in the assessment of an autoimmune disease. By using three different tissues for sampling, we had

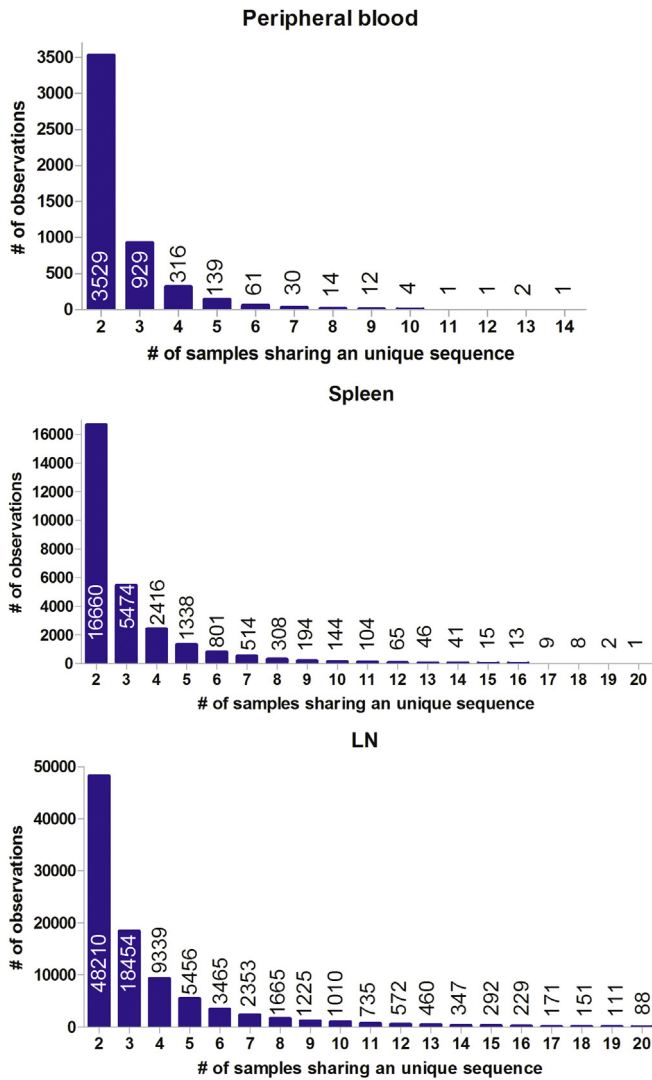


**Fig. 3. The shared unique sequences between samples.** The shared unique sequences are shown for peripheral blood, spleen and lymph node. While in peripheral blood, only 14 mice share one clone, all twenty share one clone in spleen, and 88 clones in LN.

the opportunity to investigate the relationship between putative antigen specific TCR clones in peripheral blood, spleen and lumbar lymph node.

We hypothesised that MPO immunized mice would have fewer unique clones compared to naïve mice due to loss of diversity caused by clonal expansion; however, this was not observed in any of the tissues. Rather, we saw a higher frequency of unique clones, as well as total clones, in immunized mice compared to non-immunized mice in samples from spleen and peripheral blood. This is likely to reflect a polyclonal expansion of clones towards the antigen. Although Aire  $-/-$  mice have been reported to develop a more severe induced glomerulonephritis than wt littermates, we found no differences in diversity between the Aire  $-/-$  and wt mice. This suggests a broad, polyclonal expansion towards auto-antigen, or that the autoimmune T cells reside in the affected tissues.

The impact of immunization with MPO was evident on the utilization of the V and J genes where we found a highly expanded V gene usage in the immunized mice, in particular for the V gene 13–3 in all tissues. This gene was also found in the top clones in common for the immunized mice. This highlights that expansion of specific TCR clones is detectable already with such crude

comparison between groups, but our data also shows that clones specifically expanded in response to an antigen can be impossible to identify at the level of average V gene usage, as seen in Table 2. TRVB 13–3, together with 19-0 which we also found to be expanded after immunization, are found to be expanded in NOD prediabetic and diabetic nod mice [27,28], suggesting these gene segments to be of particular interest in autoimmune diseases with possible therapeutic potential. Also, changes in gene usage could suggest a possible auto-antigen receptor motif instead of a specific highly shared TCR.

The utilization of J genes in naïve wt mice in our study were very similar to the results by Ndifon et al., where the splenic TCR $\beta$  CDR3 repertoire in five naïve C57Bl/6 mice were analysed on the RNA-level by massive parallel sequencing [29]. There were larger discrepancies regarding the V genes, and the sequences that were most highly used in our study were not amplified in Ndifon et al. [29]. A specific V and J gene usage in Aire  $-/-$  naïve mice in the C57Bl/6 background was evident in all tissues, suggesting an expansion of TCRs specific for different autoantigens, thus reflecting the loss of negative selection. Previously this repertoire has been investigated by flow cytometry and spectratyping with conflicting results [14,30], however, the reported increased usage of TRV $\beta$  19 in T cells isolated from spleen is in accordance with our results [30]. The low number of V and J gene combinations utilized in all of the LN samples from our mice suggests a biased usage of V and J genes, which is in agreement with findings in human TCR repertoires [23,31] as well as in mice [29].

The most informative comparison made available through the massive parallel sequencing of TCR $\beta$  CDR3 regions is of the unique TCR $\beta$  CDR3 sequences. Looking at the overlap of unique amino acid sequences in each tissue, it was evident that the tissue investigated and the number of T cells sequenced was of great importance, as no overlapping unique clones were found in common for all the samples from peripheral blood (Fig. 4). When we explored the overlap of unique clones from the spleen samples for the different groups of mice, we found a significantly reduced number of clones in common for immunized mice compared to naïve mice. This suggests an individual and unique response towards MPO that drives down the amount of sharing between the samples.

The TCR sequences in common for four or more mice from any of the groups were very seldom unique to that group (Supplemental Table S6). This suggests that these clones were either expanded due to immunization in common between immunized mice, due to reactivity to autoantigens in common between Aire  $-/-$  mice, or in response to an antigen in common for mice in several groups.

Aire  $-/-$  mice were expected to have more clones in common compared to wt mice, as the Aire  $-/-$  mice have the propensity to develop autoimmunity to the same autoantigens. However, examination of the number of unique clones in common among all Aire  $-/-$  samples did not identify any trend indicating a difference in the TCR repertoire compared to wt mice. When unique sequences were compared in pairs within a group, we unexpectedly found a higher number of clones in common for the naïve wt mice, both in mouse pairs and within the groups. This could reflect that the recognition of common autoantigens in the Aire  $-/-$  and the immunized mice is highly polyclonal and unique to each animal.

Comparing Aire  $-/-$  mice to wt, we identified differential usage of V genes in all tissues, as well as clones restricted to Aire  $-/-$  mice in LNs and spleen, indicating a TCR repertoire expanded in response to loss of negative selection, but this was not reflected in changes in diversity in the TCR repertoire. C57Bl/6 Aire  $-/-$  mice have previously been shown to develop autoantibodies as markers of an autoimmune reaction at 20–25 weeks of age [14], and the mice in this study (16–29 weeks of age, the majority between 16 and 17 weeks) might not have fully developed autoimmunity yet. As

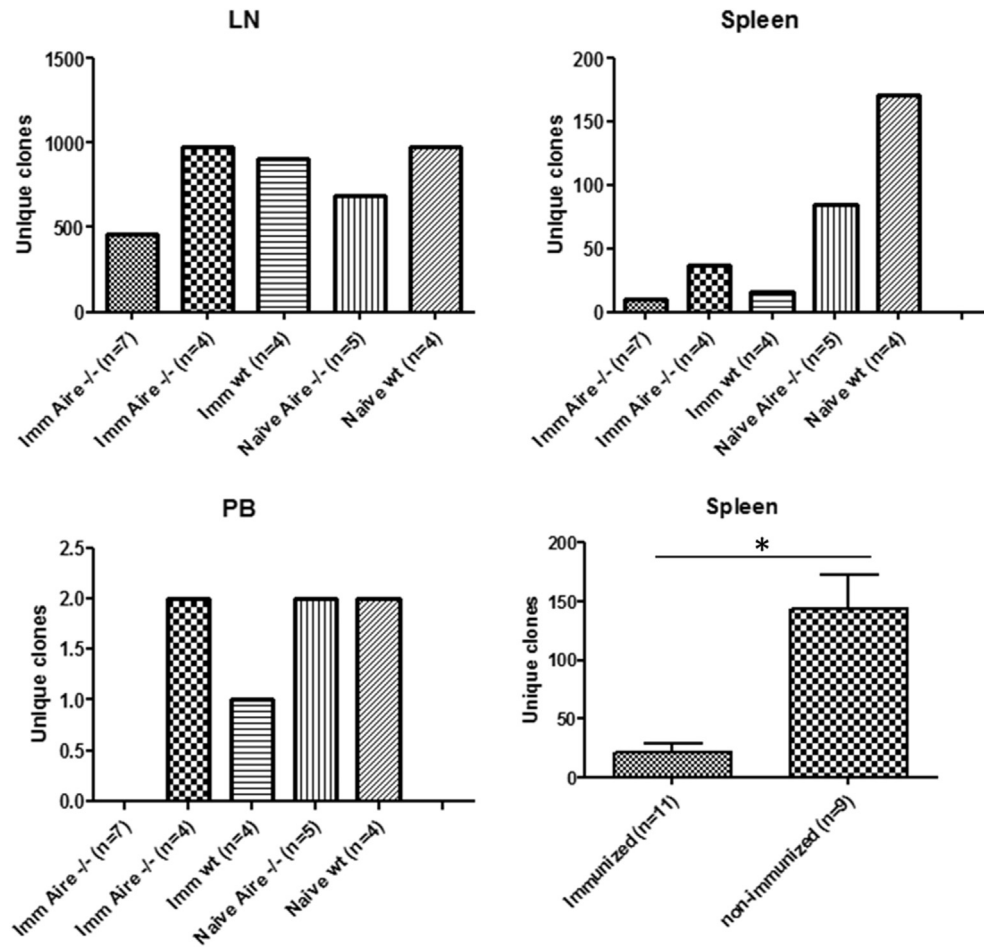


**Fig. 4. Overlapping, unique amino acid sequences between the groups.** Overlapping, unique clones were investigated in all tissues and among the immunized and non-immunized mice. The immunized mice show a significant reduction of overlapping clones. The samples were analysed using an unpaired, two-tailed *t*-test. \**p* < 0.05.

previously shown [14], there is individual variation between the mice in their recognition of autoantigens that could mask a clonal expansion within the group. It is also likely that the autoreactive T cells mainly reside in their target tissue. It could be that other functions of Aire, like Aire's involvement in the development of some thymic Treg populations [32], the extrathymic Aire-expressing cells that inactivate CD4<sup>+</sup> T cells [33] or the effect that loss of Aire has on the thymic milieu [34,35] could influence our results and be the main reason for the observed difference in V gene usage.

A very intriguing finding is the identification of TCR $\beta$  CDR3 sequences that are specifically and highly increased in all or the majority of the immunized mice but not detected in any samples from naïve wt mice (Table 2). The top clone CASSGTENTEVFF utilizing the TRBV13-1 and TRBJ1-1 genes is our best candidate for recognising MPO, and the clone CASSETENTEVFF with a single nucleotide substitution would also be expected to recognise the same antigen epitope. None of our top sequences has to our knowledge previously been described in the literature and are not present in the Genbank Mouse, the UniProt Mouse databases or the databases used by IMGT/V-QUEST. One study in humans with microscopic polyangiitis has described TCR sequences from T cell lines specific to MPO generated from peripheral T cells from patients [36]. These TCR sequences share a maximum of two amino acids with our top sequences in the amino acid sequence in the part of the CDR3 made up by the D gene and inserted nucleotides, i.e. TG or G\_E. This is in concordance with the similarities in epitope

sharing between humans and mice for autoantibody reactivity to MPO, where one of the main B cell epitopes in humans and mice also overlaps with the dominant T cell epitope in mice [37]. We find that the TCR $\beta$  sequences recognising MPO have limited sequence diversity, which could make them suitable as therapeutic targets by idiopathic TCRs, an approach that has shown to prevent allergic encephalomyelitis in mice [38], and to have beneficial effects in patients with multiple sclerosis [39,40]. Thus, further studies could possibly reveal a potential as biomarkers and therapeutic targets [3] in patients with ANCA associated vasculitis and necrotising glomerulonephritis.

So far only few studies utilize this high throughput approach to monitor autoimmune diseases. Our model system emphasises the fact that in order to reveal TCR $\beta$  sequences specific to autoantigens, one needs access to the targeted tissue or a tissue of immunological activity [27,41]. Inkludere Hayday paper her This is an obvious drawback to fully applying this method in the field of autoimmunity, as it will call for invasive surgery or post mortem assessment. However, the current effort in epitope-MHC investigations and the utilization of MHC multimer technology [42] might be useful tools in this process, shedding light on the establishment and breakdown of tolerance in autoimmune diseases as well as tissue destruction and the potential to use this information in targeted immunotherapy. More intriguingly, as studies from mice points to a limited set of TRBV genes that contribute to autoimmune disease, this could lead to new therapeutic targets and disease intervention which is still poorly described in most autoimmune disorders.



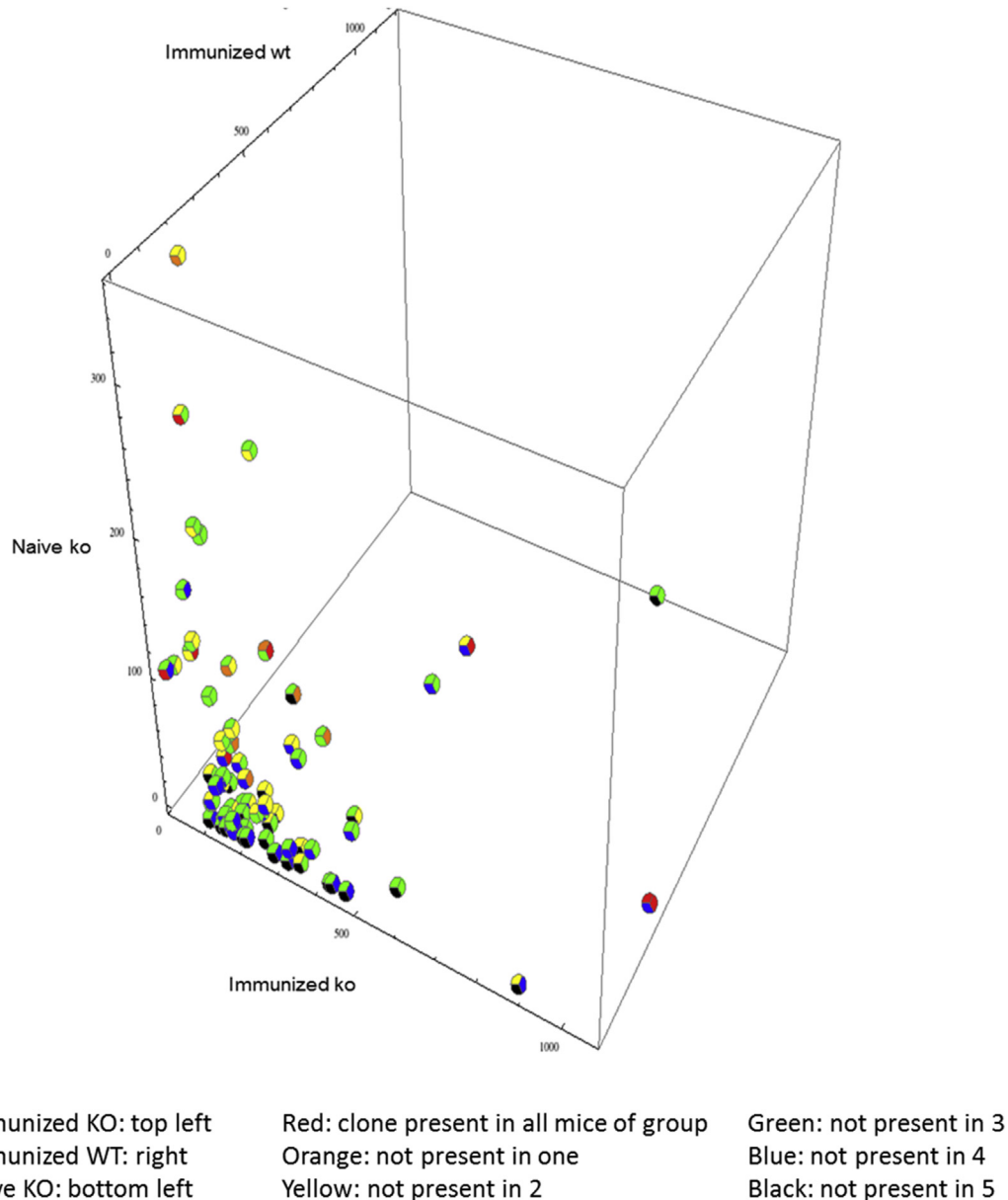


**Fig. 5. 3D plot with clones in common in LN for 4 immunized wt or more, but not in naïve wt mice.** To select clones which should be present in one or both of the immunized groups, and could be detected in naïve ko mice as they have the propensity to develop autoimmunity to this antigen, and to prioritise between the clones, a 3d-graph was produced where the average depth of clones (axes) as well as the number of samples with the clone present in the different groups (pie chart dots) was depicted. An explanation for the pie chart dots is found in the bottom of the figure. The clones to the bottom right side of the plot were of most interest since they were present at high copy numbers in immunized wt and/or ko mice but no or few copies in the naïve ko mice. Clones only present in immunized ko mice in high numbers could also be specific to MPO as this group could have a specific T cell repertoire in common.

In conclusion, using next generation sequencing, we have identified potential specific TCR $\beta$  sequences recognising MPO, and show that these sequences have limited diversity. We observe changes to the repertoire already in the utilization of V and J genes, and identified common CDR3 sequences restricted to the Aire  $-/-$  mice. However, the reaction towards shared autoantigens seems to be private and highly polyclonal, and this study emphasises the importance of the choice of tissue if utilizing this technique to monitor and diagnose autoimmune diseases.

#### Authorship contributions

BEO, BAL and HSS wrote the manuscript. CNH, BAL, PYG SRH and

HSS planned experiments. BAL and PYG performed experiments. BAL, BEO, AWS and DH performed data analysis. All authors critically reviewed and approved the manuscript.

#### Disclosure of conflicts of interest

The authors declare no conflict of interest.

#### Acknowledgements

This work was supported by a fellowship from the National Health and Medical Research Council, Australia (APP1023059) to HSS. Grants and fellowships from the Swedish Society of Medicine

SLS-96661, the Swedish Endocrine Society, and the Swedish Research Council 524-2010-6723 to BAL. Grant from the Research Council of Norway (250030) to BEO.

## Appendix A. Supplementary data

Supplementary data related to this article can be found at <http://dx.doi.org/10.1016/j.jaut.2017.03.002>.

## References

- [1] I. Kirsch, M. Vignali, H. Robins, T-cell receptor profiling in cancer, *Mol. Oncol.* 9 (2015) 2063–2070, <http://dx.doi.org/10.1016/j.molonc.2015.09.003>.
- [2] A. Mori, S. Deola, L. Xumerle, V. Mijatovic, G. Malerba, V. Monsurro, Next generation sequencing: new tools in immunology and hematology, *Blood Res.* 48 (2013) 242–249.
- [3] M. Attaf, E. Huseby, A.K. Sewell, Alphabeta T cell receptors as predictors of health and disease, *Cell Mol. Immunol.* 12 (2015) 391–399.
- [4] M.M. Davis, P.J. Bjorkman, T-cell antigen receptor genes and T-cell recognition, *Nature* 334 (1988) 395–402.
- [5] J. J. Miles, D. C. Douek, D. A. Price. Bias in the alphabeta T-cell repertoire: implications for disease pathogenesis and vaccination. *Immunol. Cell Biol.*;89: 375–387.
- [6] M.S. Anderson, E.S. Venanzi, L. Klein, Z. Chen, S.P. Berzins, S.J. Turley, et al., Projection of an immunological self shadow within the thymus by the aire protein, *Sci. (New York, NY)* 298 (2002) 1395–1401.
- [7] J. Derbinski, A. Schulte, B. Kyewski, L. Klein, Promiscuous gene expression in medullary thymic epithelial cells mirrors the peripheral self, *Nat. Immunol.* 2 (2001) 1032–1039.
- [8] N. Kuroda, T. Mitani, N. Takeda, N. Ishimaru, R. Arakaki, Y. Hayashi, et al., Development of autoimmunity against transcriptionally unrepressed target antigen in the thymus of Aire-deficient mice, *J. Immunol.* 174 (2005) 1862–1870.
- [9] An autoimmune disease, APECED, caused by mutations in a novel gene featuring two PHD-type zinc-finger domains, *Nat. Genet.* 17 (1997) 399–403.
- [10] K. Nagamine, P. Peterson, H.S. Scott, J. Kudoh, S. Minoshima, M. Heino, et al., Positional cloning of the APECED gene, *Nat. Genet.* 17 (1997) 393–398.
- [11] O. Bruslerud, B.E. Oftedal, N. Landegren, M. Erichsen, E. Bratland, K. Lima, et al., A longitudinal follow-up of Autoimmune polyendocrine syndrome type 1, *J. Clin. Endocrinol. Metab.* 101 (8) (2016 Aug.), 2975–2983, <http://dx.doi.org/10.1210/jc.2016-1821>.
- [12] E.M. Ferre, S.R. Rose, S.D. Rosenzweig, P.D. Burbelo, K.R. Romito, J.E. Niemela, et al., Redefined clinical features and diagnostic criteria in autoimmune polyendocrinopathy-candidiasis-ectodermal dystrophy, *JCI Insight* (2016) 1.
- [13] S. Meyer, M. Woodward, C. Hertel, P. Vlaicu, Y. Haque, J. Karner, et al., AIRE-deficient patients harbor unique high-affinity disease-ameliorating autoantibodies, *Cell* 166 (2016) 582–595.
- [14] F.X. Hubert, S.A. Kinkel, P.E. Crewther, P.Z. Cannon, K.E. Webster, M. Link, et al., Aire-deficient C57BL/6 mice mimicking the common human 13-base pair deletion mutation present with only a mild autoimmune phenotype, *J. Immunol.* 182 (2009) 3902–3918.
- [15] D. S. Tan, P. Y. Gan, K. M. O'Sullivan, M. V. Hammett, S. A. Summers, J. D. Ooi et al. Thymic deletion and regulatory T cells prevent antimyelo-peroxidase GN. *J. Am. Soc. Nephrol.*;24:573–585.
- [16] H. Xiao, P. Heeringa, P. Hu, Z. Liu, M. Zhao, Y. Aratani, et al., Antineutrophil cytoplasmic autoantibodies specific for myeloperoxidase cause glomerulonephritis and vasculitis in mice, *J. Clin. Invest.* 110 (2002) 955–963.
- [17] P. Y. Gan, S. R. Holdsworth, A. R. Kitching, J. D. Ooi. Myeloperoxidase (MPO)-specific CD4+ T cells contribute to MPO-anti-neutrophil cytoplasmic antibody (ANCA) associated glomerulonephritis. *Cell. Immunol.*;282:21–27.
- [18] A.J. Ruth, A.R. Kitching, R.Y. Kwan, D. Odobasic, J.D. Ooi, J.R. Timoshanko, et al., Anti-neutrophil cytoplasmic antibodies and effector CD4+ cells play nonredundant roles in anti-myeloperoxidase crescentic glomerulonephritis, *J. Am. Soc. Nephrol.* 17 (2006) 1940–1949.
- [19] J. D. Ooi, J. Chang, M. J. Hickey, D. B. Borza, L. Fugger, S. R. Holdsworth et al. The immunodominant myeloperoxidase T-cell epitope induces local cell-mediated injury in antimyelo-peroxidase glomerulonephritis. *Proc. Natl. Acad. Sci. U. S. A.*;109:E2615–E2624.
- [20] S.A. Summers, O.M. Steinmetz, M. Li, J.Y. Kausman, T. Semple, K.L. Edgton, et al., Th1 and Th17 cells induce proliferative glomerulonephritis, *J. Am. Soc. Nephrol.* 20 (2009) 2518–2524.
- [21] P. Y. Gan, O. M. Steinmetz, D. S. Tan, K. M. O'Sullivan, J. D. Ooi, Y. Iwakura et al. Th17 cells promote autoimmune anti-myeloperoxidase glomerulonephritis. *J. Am. Soc. Nephrol.*;21:925–931.
- [22] J. Apostolopoulos, J.D. Ooi, D. Odobasic, S.R. Holdsworth, A.R. Kitching, The isolation and purification of biologically active recombinant and native autoantigens for the study of autoimmune disease, *J. Immunol. methods* 308 (2006) 167–178.
- [23] H.S. Robins, P.V. Campregher, S.K. Srivastava, A. Wacher, C.J. Turtle, O. Khsai, et al., Comprehensive assessment of T-cell receptor beta-chain diversity in alphabeta T cells, *Blood* 114 (2009) 4099–4107.
- [24] M. Yousfi Monod, V. Giudicelli, D. Chaume, M.P. Lefranc, IMGT/JunctionAnalysis: the first tool for the analysis of the immunoglobulin and T cell receptor complex V-J and V-D-J JUNCTIONS, *Bioinforma. Oxf. Engl.* 20 (Suppl 1) (2004) i379–85.
- [25] S.F. Altschul, W. Gish, W. Miller, E.W. Myers, D.J. Lipman, Basic local alignment search tool, *J. Mol. Biol.* 215 (1990) 403–410.
- [26] X. Brochet, M.P. Lefranc, V. Giudicelli, IMGT/V-QUEST: the highly customized and integrated system for IG and TR standardized V-J and V-D-J sequence analysis, *Nucleic acids Res.* 36 (2008) W503–W508.
- [27] I. Marrero, D. E. Hamm, J. D. Davies. High-throughput sequencing of islet-infiltrating memory CD4(+) T cells reveals a similar pattern of TCR beta usage in prediabetic and diabetic nod mice. *PLoS One*;8:e76546.
- [28] R. Toivonen, T.P. Arstila, A. Hanninen, Islet-associated T-cell receptor-beta CDR sequence repertoire in prediabetic NOD mice reveals antigen-driven T-cell expansion and shared usage of Vbeta4beta TCR chains, *Mol. Immunol.* 64 (2015) 127–135.
- [29] W. Ndiifon, H. Gal, E. Shifrut, R. Aharoni, N. Yissachar, N. Waysbort et al. Chromatin conformation governs T-cell receptor beta gene segment usage. *Proc. Natl. Acad. Sci. U. S. A.*;109:15865–15870.
- [30] C. Ramsey, O. Winqvist, L. Puhakka, M. Halonen, A. Moro, O. Kampe, et al., Aire deficient mice develop multiple features of APECED phenotype and show altered immune response, *Hum. Mol. Genet.* 11 (2002) 397–409.
- [31] H. S. Robins, S. K. Srivastava, P. V. Campregher, C. J. Turtle, J. Andriesen, S. R. Riddell et al. Overlap and effective size of the human CD8+ T cell receptor repertoire. *Sci. Transl. Med.*;2:47ra64.
- [32] S. Malchow, D. S. Leventhal, S. Nishi, B. I. Fischer, L. Shen, G. P. Paner et al. Aire-dependent thymic development of tumor-associated regulatory T cells. *Sci. New York, N. Y.*;339:1219–1224.
- [33] J. M. Gardner, T. C. Metzger, E. J. McMahon, B. B. Au-Yeung, A. K. Krawisz, W. Lu et al. Extrathymic Aire-expressing cells are a distinct bone marrow-derived population that induce functional inactivation of CD4(+) T cells. *Immunity*;39: 560–572.
- [34] J. E. Cowan, S. M. Parnell, K. Nakamura, J. H. Caamano, P. J. Lane, E. J. Jenkinson et al. The thymic medulla is required for Foxp3+ regulatory but not conventional CD4+ thymocyte development. *J. Exp. Med.*;210:675–681.
- [35] M. Hinterberger, M. Aichinger, O. Prazeres da Costa, D. Voehringer, R. Hoffmann, L. Klein. Autonomous role of medullary thymic epithelial cells in central CD4(+) T cell tolerance. *Nat. Immunol.*;11:512–519.
- [36] N. Seta, S. Kobayashi, H. Hashimoto, M. Kuwana, Characterization of autoreactive T-cell clones to myeloperoxidase in patients with microscopic polyangiitis and healthy individuals, *Clin. Exp. Rheumatol.* 27 (2009) 826–829.
- [37] A. J. Roth, J. D. Ooi, J. J. Hess, M. M. van Timmeren, E. A. Berg, C. E. Poulton et al. Epitope specificity determines pathogenicity and detectability in ANCA-associated vasculitis. *J. Clin. Invest.*;123:1773–1783.
- [38] H. Offner, G.A. Hashim, A.A. Vandenbark, T cell receptor peptide therapy triggers autoregulation of experimental encephalomyelitis, *Sci. New York, N. Y.* 251 (1991) 430–432.
- [39] E.E. Morgan, C.J. Nardo, J.P. Diveley, J. Kunin, R.M. Bartholomew, R.B. Moss, et al., Vaccination with a CDR2 BV6S2/6S5 peptide in adjuvant induces peptide-specific T-cell responses in patients with multiple sclerosis, *J. Neurosci. Res.* 64 (2001) 298–301.
- [40] D.P. Gold, R.A. Smith, A.B. Golding, E.E. Morgan, T. Dafashy, J. Nelson, et al., Results of a phase I clinical trial of a T-cell receptor vaccine in patients with multiple sclerosis. II. Comparative analysis of TCR utilization in CSF T-cell populations before and after vaccination with a TCRV beta 6 CDR2 peptide, *J. Neuroimmunol.* 76 (1997) 29–38.
- [41] D.R. Thapa, R. Tonikian, C. Sun, M. Liu, A. Dearth, M. Petri, et al., Longitudinal analysis of peripheral blood T cell receptor diversity in patients with systemic lupus erythematosus by next-generation sequencing, *Arthritis Res. Ther.* 17 (2015) 132.
- [42] G. Dolton, K. Tungatt, A. Lloyd, V. Bianchi, S.M. Theaker, A. Trimby, et al., More tricks with tetramers: a practical guide to staining T cells with peptide-MHC multimers, *Immunology* 146 (2015) 11–22.